Theoretical studies on the protonation behavior of tropone and its metal complexes

Alireza Ariafard, Zhenyang Lin *

Department of Chemistry, The Hong Kong University of Science and Technology, Clear Water Bay, Kowloon, Hong Kong

Abstract

Density functional theory calculations were carried out to investigate structures and stabilities of tropone and troponeiron complexes, (tropone)Fe(CO)$_3$, (tropone)Fe(CO)$_2$(PH$_3$) and (tropone)Fe(PH$_3$)$_3$, and their protonated species. The results show that the oxygen-protonated tropone is more stable than the carbon-protonated tropone. On the contrary, in the troponeiron complexes, the carbon protonated species are more stable than the oxygen protonated species. In the neutral and oxygen-protonated complexes, the tropone and oxygen-protonated tropone ligands are η^4-coordinated. In the carbon-protonated complexes, the carbon-protonated tropone ligand is η^5-coordinated. The results also show that the metal shift for complexes containing phosphine ligands is more difficult than that for those containing carbonyl ligands. For the neutral methyl-substituted troponeiron complexes, steric effect was found to play a key role in determining the relative stability of the regioisomers. For their protonated species, the electron-donating properties of the methyl substituent(s) were found to be important in determining the relative stability among the different regioioismers.
© 2005 Elsevier B.V. All rights reserved.

Keywords: Tropone; Tropone complexes; Protonation of tropone and its metal complexes; Density functional theory calculations

1. Introduction

Tropones (**1**) and troponeiron complexes (**2**) have received considerable attention because they are important intermediates for cycloaddition reactions and synthesis of heterocyclic compounds [1]. Protonation of such compounds due to their importance in synthesizing other organic compounds has also attracted interest. Studies show that protonation of the tropone complexes (**2**) followed by reaction with Na$_2$CO$_3$/ROH yields alkyl ethers (**3**) [2–4].


1   **2**   **3**

(L)$_3$ = (CO)$_3$ *or* (CO)$_2$(PPh$_3$)
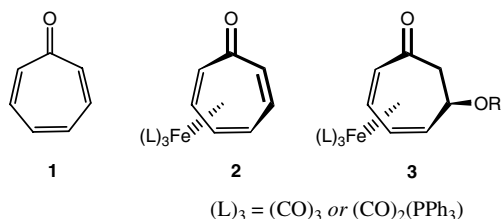
Protonation of free tropones was found to take place at oxygen (**1_OH**$^+$) [5]. The protonated species (**1_OH**$^+$) has a pK_a value of −1.02, indicating that tropones are much more basic than typical ketones [6]. Interestingly, as early as 1970s, it was well established that protonation of troponeiron complexes is kinetically controlled at oxygen giving hydroxytropyliumiron cationic complexes [7]. These oxygen-protonated complexes upon either standing for several minutes or increasing temperature isomerize to thermodynamically more stable carbon-protonated pentadienyliron cationic complexes (**2_CH**$^+$) [7–9].

1_OH$^+$ **2_CH**$^+$
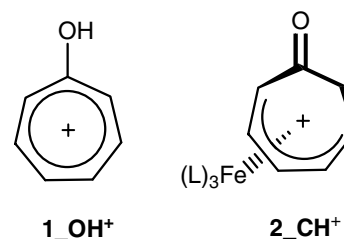
* Corresponding author.
 E-mail address: chzlin@ust.hk (Z. Lin).

Experimental studies also demonstrated that substituents on the tropone ring influence the relative stability of regioisomers of the protonated troponeiron complexes as well as the barriers to their interconversion [2,4,7]. For example, NMR studies of 2-methyltroponeiron complexes indicated that regioisomer **4** was thermodynamically more stable than regioisomer **4′**. Protonation and then neutralization with a weak base gave a mixture enriched with the less favorable regioisomer **4′**. These experimental results show that the protonated species of regioisomer **4′** could be more stable than the protonated species of regioisomer **4** although the neutral regioisomer **4** is more stable than the neutral regioisomer **4′**. Also, studies on the fluxionality of 2-methyltroponeiron complexes indicated that the barrier to the interconversion between **4** and **4′** is also different from the barrier to the interconversion between their protonated species [2,4,7]. Similar observations also hold true for 2,6-dimethyltroponeiron complexes having two methyl groups on the tropone ring, i.e., **5** is more stable than **5′** while the stability order of their protonated species is reversed [2].
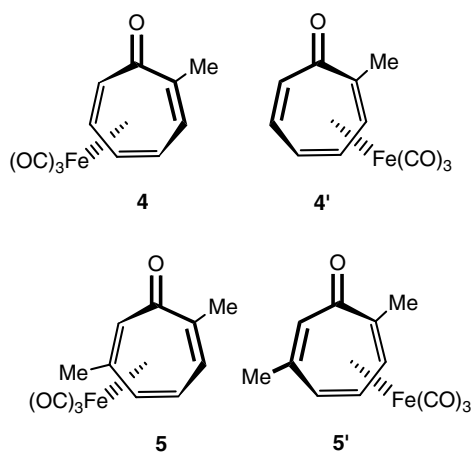
The main goals of the present study are to theoretically investigate relative stabilities of the carbon-protonated pentadienyliron cationic complexes and hydroxytropylium-iron cationic complexes and to understand how protonation of troponeiron complexes alters the relative stabilities of the regioisomers as well as the barriers to their interconversion.

2. Computational details

All structures were fully optimized at the B3LYP level of the density functional theory [10], and then frequencies were analytically computed at the same level of theory to examine whether the optimized structures are minima or transition states. The 6-31G basis set [11] was employed for C, O, and H atoms. The effective core potentials of Hay and Wadt with double-ζ valance basis sets (LanL2DZ) [12] were used for Fe and P. Polarization functions were also added for C ($\zeta_d = 0.6$), O ($\zeta_d = 1.154$), P ($\zeta_d = 0.340$), and Fe ($\zeta_f = 2.462$) [13,14]. To confirm that

the calculated transition states are indeed connecting two minima, calculations of intrinsic reaction coordinates (IRC) were performed [15]. Partial atomic charges were calculated on the basis of the natural bond orbital (NBO) analyses [16]. To estimate the degree of aromaticity of the tropone and the protonated tropones, nucleus independent chemical shift (NICS) calculations [17] were performed using the GIAO method [18] and the B3LYP/6-311G(d,p) wavefunctions. NICS(0) values were calculated at the center of the ring, found by averaging the coordinates of the six atoms forming the ring. NICS(1) values were calculated at a point 1 Å away from the center of the ring, in a direction perpendicular to the plane of the ring.

To examine the effect of basis sets, we also employed a larger basis set, which has SDDAll [19] for Fe and 6-311G** for all other atoms, to perform single-point energy calculations for several selected structures. The additional calculations show that the basis set dependence is small. For example, using the smaller basis set, the relative energies of **4**, **4Ts** and **4′** are 0.0, 19.9 and 3.6 kcal/mol, respectively. Using the larger basis set, the relative energies of **4**, **4Ts** and **4′** are 0.0, 18.1 and 3.7 kcal/mol, respectively. Similarly, using the smaller basis set, the relative energies of **5**, **5Ts** and **5′** are 0.0, 20.1 and 2.9 kcal/mol, respectively. Using the larger basis set, the relative energies of **5**, **5Ts** and **5′** are 0.0, 18.7 and 3.3 kcal/mol, respectively. All the calculations were performed by GAUSSIAN 03 package [20].

3. Results and discussion

3.1. Structures and stabilities of tropone, troponeiron complexes and their protonated species

As mentioned in the Introduction, the free tropone is preferentially protonated at the oxygen atom while the troponeiron complexes undergo protonation at carbon thermodynamically. Figs. 1 and 2 show the calculated geometries and the corresponding relative energies of both the oxygen- and carbon-protonated species of tropone and the model troponeiron complexes (tropone)Fe(CO)$_3$, (tropone)Fe(CO)$_2$(PH$_3$) and (tropone)Fe(PH$_3$)$_3$, respectively. The results of the calculations indicate that, consistent with the experimental findings, the hydroxytropylium cation **1_OH**$^+$ is more stable than the carbon-protonated pentadienyl cation **1_CH**$^+$ while the hydroxytropylium cationic iron complexes, **2CO_OH**$^+$, **2COPH3_OH**$^+$ and **2PH3_OH**$^+$, are less stable than the carbon-protonated pentadienyl cationic iron complexes, **2CO_CH**$^+$, **2COPH3_CH**$^+$ and **2PH3_CH**$^+$, respectively.

The model complex (tropone)Fe(CO)$_2$(PH$_3$) can adopt different structural isomers considering the orientation of the Fe(CO)$_2$(PH$_3$) fragment with respect to the tropone ring. For convenience, we calculated the structural isomer found in the crystal structure of (tropone)Fe(CO)$_2$(PPh$_3$) [3]. The same orientation of the Fe(CO)$_2$(PH$_3$) fragment was employed in the calculation of the corresponding

1

1_OH⁺
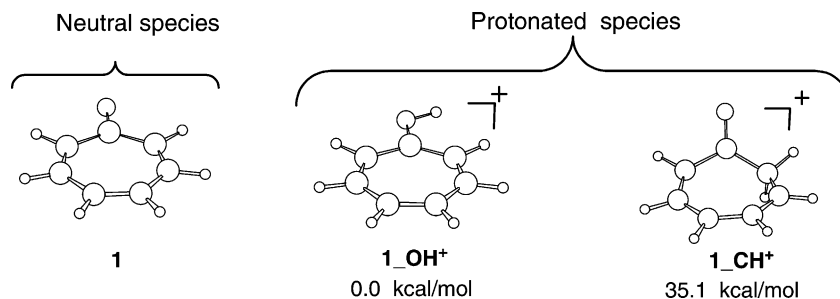0.0 kcal/mol

1_CH⁺
35.1 kcal/mol

Fig. 1. Optimized structures of tropone and its protonated species.

oxygen- and carbon-protonated species. Neglect of other structural isomers should not affect the conclusions we are going to make. We are mainly concerned about how the number of phosphine ligands influences the relative stability of the oxygen- and carbon-protonated species. This is reason that we also calculated the model complex (tropone)Fe(PH₃)₃ and its corresponding oxygen- and carbon-protonated species.

The much higher stability of **1_OH⁺** relative to **1_CH⁺** is a result of aromaticity in **1_OH⁺**. We calculated NICS values to estimate the degree of aromaticity of these species. The NICS values are calculated at 0.0, NICS(0) and 1.0 Å, NICS(1), above the molecular plane. The NICS(0) [NICS(1.0)] values of 1.2 [−2.6], −5.3 [−8.2], 4.6 [0.1] were calculated for **1**, **1_OH⁺**, and **1_CH⁺**, respectively. Thus, **1_OH⁺** is aromatic, while **1_CH⁺** is non-aromatic. The higher stability of **1_OH⁺** is a result of its high degree of aromaticity, which has a large π-conjugation. Havenith et al. reported NICS for **1**, also suggesting that **1** has low aromaticity [21]. The low aromaticity of **1** is probably due to the fact that Lewis structure **1a** has small contribution to the resonance hybrid (**A**) [22].
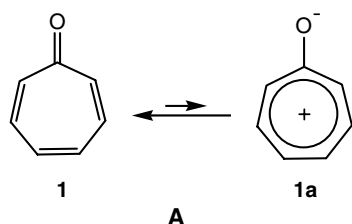
As shown in Fig. 2, the troponeiron complexes **2CO**, **2COPH3** and **2PH3** can be described as having square pyramidal structures in which one of the carbonyl or phosphine ligands occupies the apical position if the η⁴-tropone ligand is considered to occupy two basal coordination sites. The geometries around the metal centers for the oxygen-protonated species **2CO_OH⁺**, **2COPH3_OH⁺** and **2PH3_OH⁺** are almost identical to those for the neutral, unprotonated species **2CO**, **2COPH3** and **2PH3** in which the protonated tropone ligands are η⁴-coordinated. An η⁵-tropone coordination for the oxygen-protonated species could not be found. On the contrary, for the carbon-

protonated species **2CO_CH⁺**, **2COPH3_CH⁺** and **2PH3_CH⁺**, η⁵-coordination was found. The Fe–C6 bond lengths in the carbon-protonated species, as compared to those in the neutral species **2CO**, **2COPH3** and **2PH3**, are shortened by about 0.7 Å.

In all the troponeiron complexes, coordination of tropone to the metal center is concomitant with a folding of the tropone ring. Thus, one would expect that electronic factors other than aromaticity are responsible for higher stability of the carbon-protonated versus oxygen-protonated complexes. To explain the reason why the stabilities of the carbon-protonated complexes are considerably higher than those of the oxygen-protonated complexes, we analyzed the HOMOs and LUMOs of the free and protonated tropones (**1**, **1_OH⁺**, and **1_CH⁺**) and the metal fragment Fe(CO)₃. From the relative orbital energies, we can see that the HOMO and the LUMO are stabilized from **1** to **1_OH⁺** and then to **1_CH⁺** (Fig. 3). On the basis of the HOMO and LUMO orbital energies of the three ligands, we can conclude that **1_CH⁺** is the best electron accepting ligand and **1** is the best donating ligand. The NBO charge distribution calculated for the nine structures, shown in Fig. 2, of the iron complexes supports the argument here. The formally neutral tropone ligands in **2CO**, **2COPH3** and **2PH3** carry negative charges, indicating that the ligands are electron acceptors (Table 1). The protonated tropone ligands in the protonated complexes carry a charge much smaller than +1, indicating that the protonated tropone ligand gains electrons upon metal coordination. For example, the charges of the protonated tropone ligands in **2CO_OH⁺** and **2CO_CH⁺** are +0.484 and +0.312, respectively, implying that they gain 0.516 e and 0.688 e from the metal fragments upon metal-coordination.

The electrons gained by the protonated tropone ligands in the protonated complexes are considerably more than the electrons gained by the tropone ligands in the neutral complexes. These results indicate that, consistent with the LUMO energies, the electron transfer from the metal fragment to the tropone ligand or protonated tropone ligand increases in the order of the troponeiron complexes < the oxygen-protonated troponeiron complexes < the carbon protonated troponeiron complexes. The trend finds further support from the calculated CO stretching frequencies. The CO stretching frequencies calculated for the three carbonyl complexes are given below: 2095, 2103, 2142 cm⁻¹ for
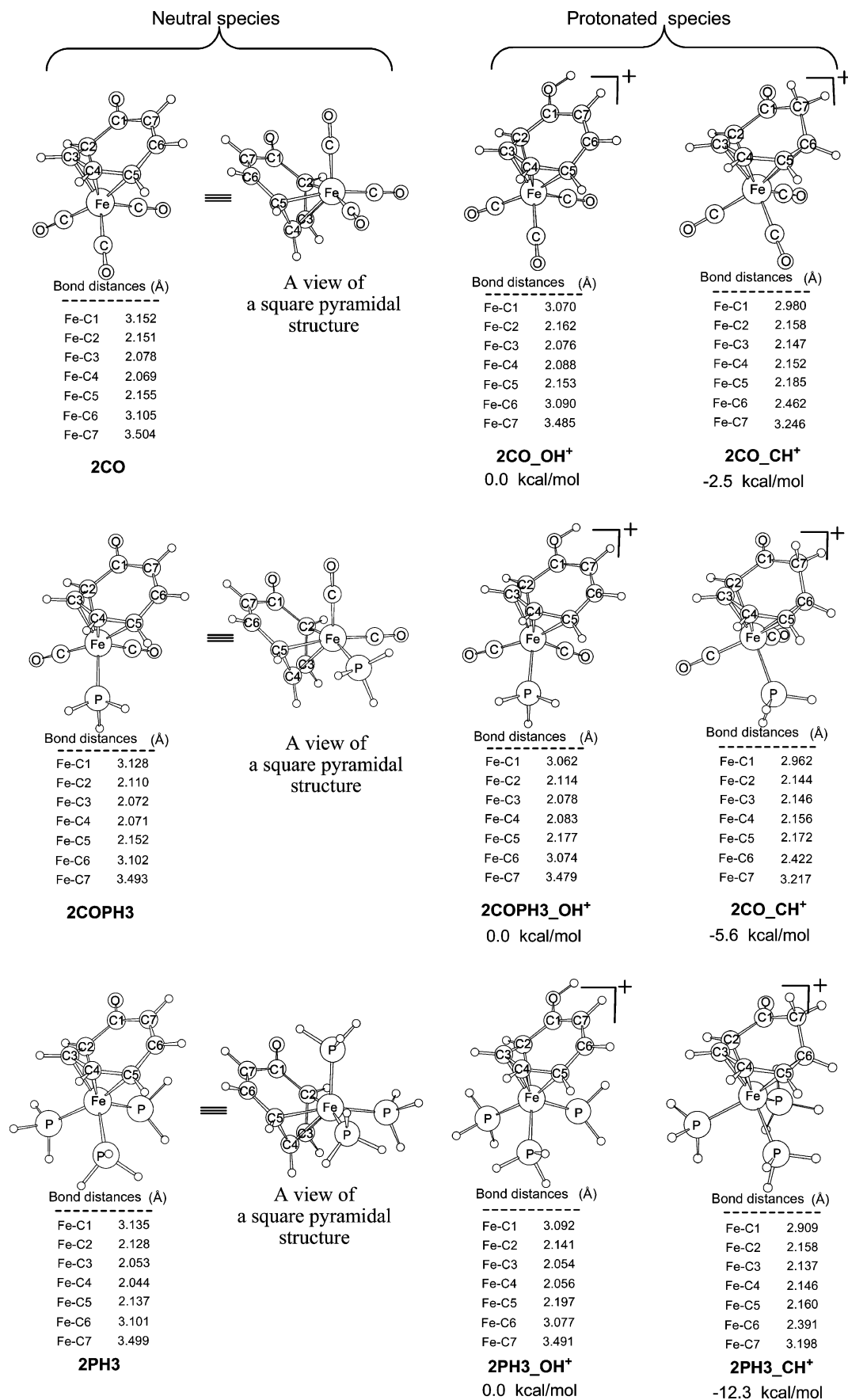
Neutral species   Protonated species

Bond distances (Å)

Fe-C1	3.152
Fe-C2	2.151
Fe-C3	2.078
Fe-C4	2.069
Fe-C5	2.155
Fe-C6	3.105
Fe-C7	3.504

2CO

A view of
a square pyramidal
structure

Bond distances (Å)

Fe-C1	3.070
Fe-C2	2.162
Fe-C3	2.076
Fe-C4	2.088
Fe-C5	2.153
Fe-C6	3.090
Fe-C7	3.485

2CO_OH$^+$
0.0 kcal/mol

Bond distances (Å)

Fe-C1	2.980
Fe-C2	2.158
Fe-C3	2.147
Fe-C4	2.152
Fe-C5	2.185
Fe-C6	2.462
Fe-C7	3.246

2CO_CH$^+$
-2.5 kcal/mol

Bond distances (Å)

Fe-C1	3.128
Fe-C2	2.110
Fe-C3	2.072
Fe-C4	2.071
Fe-C5	2.152
Fe-C6	3.102
Fe-C7	3.493

2COPH3

A view of
a square pyramidal
structure

Bond distances (Å)

Fe-C1	3.062
Fe-C2	2.114
Fe-C3	2.078
Fe-C4	2.083
Fe-C5	2.177
Fe-C6	3.074
Fe-C7	3.479

2COPH3_OH$^+$
0.0 kcal/mol

Bond distances (Å)

Fe-C1	2.962
Fe-C2	2.144
Fe-C3	2.146
Fe-C4	2.156
Fe-C5	2.172
Fe-C6	2.422
Fe-C7	3.217

2CO_CH$^+$
-5.6 kcal/mol

Bond distances (Å)

Fe-C1	3.135
Fe-C2	2.128
Fe-C3	2.053
Fe-C4	2.044
Fe-C5	2.137
Fe-C6	3.101
Fe-C7	3.499

2PH3

A view of
a square pyramidal
structure

Bond distances (Å)

Fe-C1	3.092
Fe-C2	2.141
Fe-C3	2.054
Fe-C4	2.056
Fe-C5	2.197
Fe-C6	3.077
Fe-C7	3.491

2PH3_OH$^+$
0.0 kcal/mol

Bond distances (Å)

Fe-C1	2.909
Fe-C2	2.158
Fe-C3	2.137
Fe-C4	2.146
Fe-C5	2.160
Fe-C6	2.391
Fe-C7	3.198

2PH3_CH$^+$
-12.3 kcal/mol

Fig. 2. Optimized structures of troponeiron complexes and their protonated species.
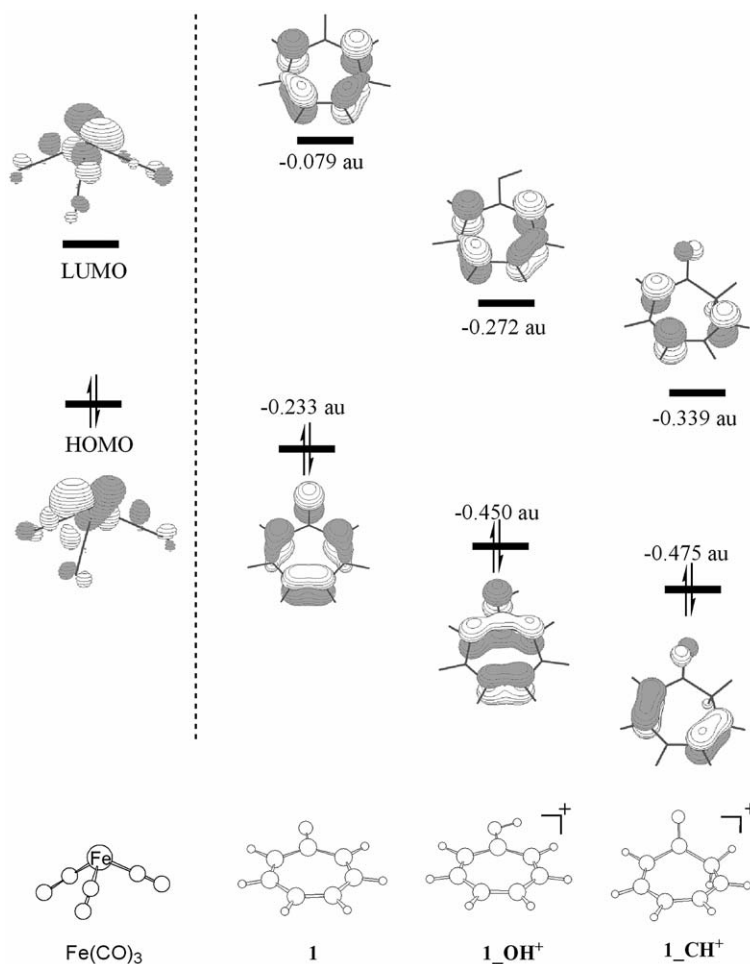
Fig. 3. The frontier orbitals of $Fe(CO)_3$, tropone and its protonated species.

Table 1
Partial charges calculated for Fe, tropone, and protonated tropone in various troponeiron complexes on the basis of the natural bond orbital (NBO) analysis

Complexes	NBO charge	
	Fe	The tropone or protonated tropone ligand
2CO	−0.293	−0.194
2COPH3	−0.287	−0.281
2PH3	−0.274	−0.475
2CO_OH+	−0.201	0.484
2CO_CH+	−0.172	0.312
2COPH3_OH+	−0.178	0.387
2COPH3_CH+	−0.161	0.217
2PH3_OH+	−0.098	0.178
2PH3_CH+	−0.094	−0.004

2CO; 2157, 2162, 2192 cm^{-1} for **2CO_OH+**; 2184, 2186, 2212 cm^{-1} for **2CO_CH+**. These results demonstrate that, consistent with the trend mentioned above, the extent of the metal(d)-to-tropone (π^*) back-bonding interaction increases in the order of **2CO < 2CO_OH+ < 2CO_CH+**.

The charge carried by the tropone ligand or the protonated tropone ligand in a given phosphine complex is more negative or less positive than that in the analogous carbonyl complex. This result suggests that the electron transfer from the metal fragment to the tropone ligands is more significant in the phosphine complexes. In the carbonyl complexes, the metal(d)-to-tropone (π^*) back-donation is decreased because of the presence of the strong π-accepting carbonyl ligands, as evidenced by the fact that the Fe–C(tropone) bond distances in the carbonyl complexes are generally longer than those in the phosphine analogues (Fig. 2).

The claim that **1_CH+** is a stronger π-acceptor ligand than **1_OH+** also finds support from the partial charges calculated for Fe, given in Table 1. For instance, the metal center Fe in **2CO_CH+** carries a smaller negative charge (−0.172) in comparison with the partial charge of −0.201 in **2CO_OH+**. The same trend is also observed between the carbon- and oxygen-protonated species of other complexes (Table 1).

Examining the frontier molecular orbitals plotted in Fig. 3, one can easily find that the symmetry characteristics of the frontier orbitals for the tropone and oxygen-protonated tropone ligands are nearly the same. The orbital symmetries for the carbon-protonated tropone ligand are, however, quite different. Clearly, the different symmetry

characteristics in the frontier orbitals explain the different coordination modes adopted by the oxygen-protonated and carbon-protonated tropone ligands. In summary, the greater delocalization of the positive charge over the metal fragments FeL$_3$ as well as the η^5-coordination of the carbon-protonated tropone ligand leads to stronger metal–tropone bonding interactions in the carbon-protonated iron complexes.

One of the reviewers suggested us to do calculations on (tropone)Fe(CO)(PH$_3$)$_2$ to have a complete set of systems (tropone)Fe(CO)$_{3-x}$(PH$_3$)$_x$ ($x = 0, 1, 2, 3$). The three isomers optimized for (tropone)Fe(CO)(PH$_3$)$_2$ have similar stability although the one having the carbonyl ligand occupying the apical position is the least stable (Fig. 4a). The result is consistent with the early finding that in d^8 complexes adopting square pyramidal structures electron π-acid ligands such as carbonyl prefer to occupy basal positions to help stabilize the HOMO through back-bonding interaction [23]. We compared the relative stability of the oxygen- and carbon-protonated species of the most stable isomer (Fig. 4b). The carbon-protonated species is calculated to be more stable than oxygen-protonated species by 9.6 kcal/mol. The net charge transfers to the tropone and protonated tropone ligands are 0.388 e, 0.718 e, and 0.917 e for the neutral, oxygen-protonated and carbon-protonated species, respectively. These results show the same trend discussed above.

3.2. Fluxionality of troponeiron complexes and their protonated species

Experimentally, it was also found that the troponeiron complexes can undergo 1,3 metal shift, i.e., π-bond migration through an η^2-coordinated unsaturated transition state [24]. Indeed, our calculations show that **2** and **2′** are connected via the transition state **2Ts**. Fig. 5 shows the energy profiles calculated for the 1,3 metal shift for the tro-
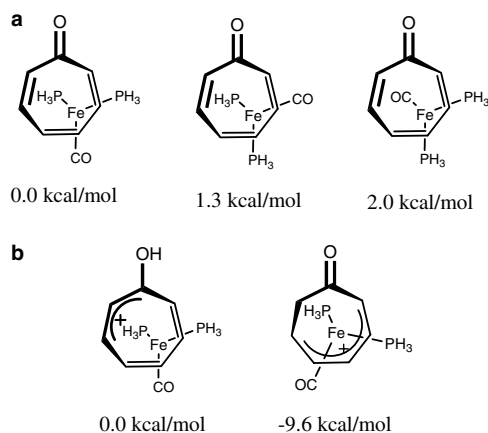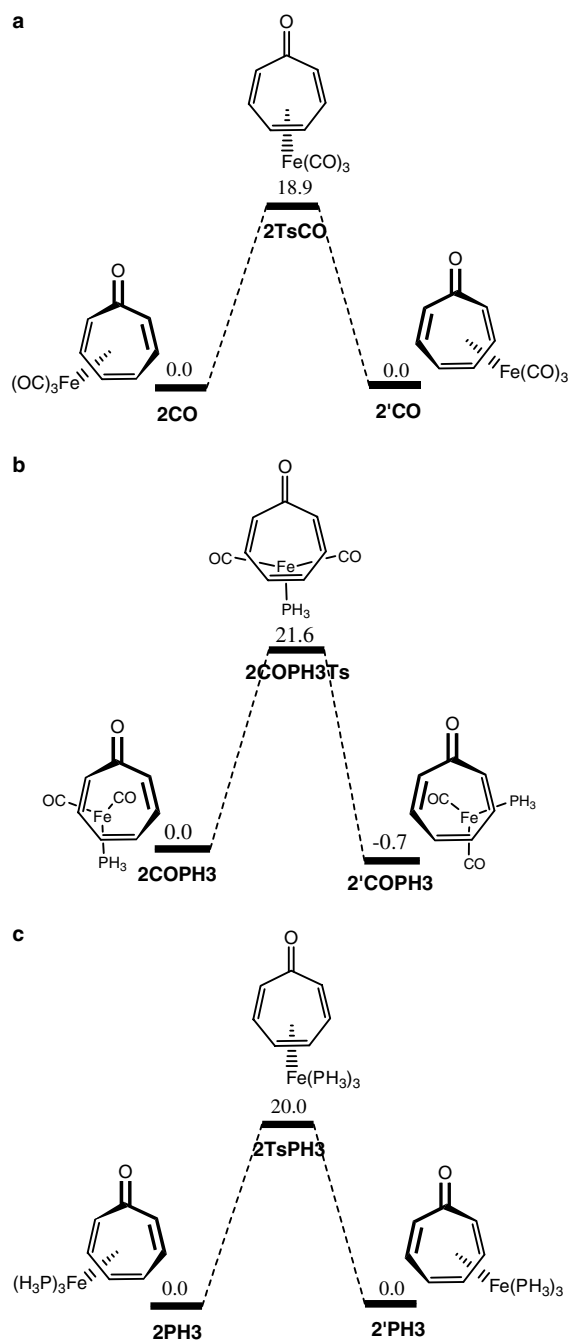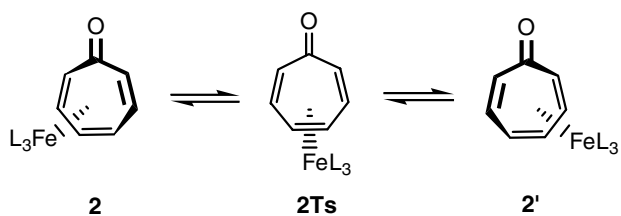
Fig. 5. Energy profiles of the 1,3 metal shifts for troponeiron complexes. The relative energies are given in kcal/mol.

poneiron complexes (tropone)Fe(CO)$_3$, (tropone)Fe(CO)$_2$-(PH$_3$) and (tropone)Fe(PH$_3$)$_3$. From Fig. 5, one can easily find that the energy barriers of the 1,3 metal shifts for all the complexes are comparable. The calculation underestimates the barrier for (tropone)Fe(CO)$_3$ by roughly 6.2 kcal/mol when compared with the experimentally measured barrier of 25.1 kcal/mol reported by Tajiri et al. [25] and our calculated barrier is very close to the one (21.2 kcal/mol) computed by González-Blanco and Branchadell [26].

Fig. 4. (a) The three isomers calculated for (tropone)Fe(CO)(PH$_3$)$_2$. (b) The oxygen-protonated and carbon-protonated species based on the most stable isomer of (tropone)Fe(CO)(PH$_3$)$_2$.

In comparison with the neutral troponeiron complexes, the energy barrier corresponding to the 1,3 metal shifts of the oxygen protonated troponeiron complexes $2CO\_OH^+$, $2COPH3\_OH^+$ and $2PH3\_OH^+$ are lowered by 3.6, 3.4 and 6.7 kcal/mol, respectively (Fig. 6). The oxygen-protonated tropone ligands in the transition states $2TsCO\_OH^+$ and $2TsCOPH3\_OH^+$, similar to those in the transition
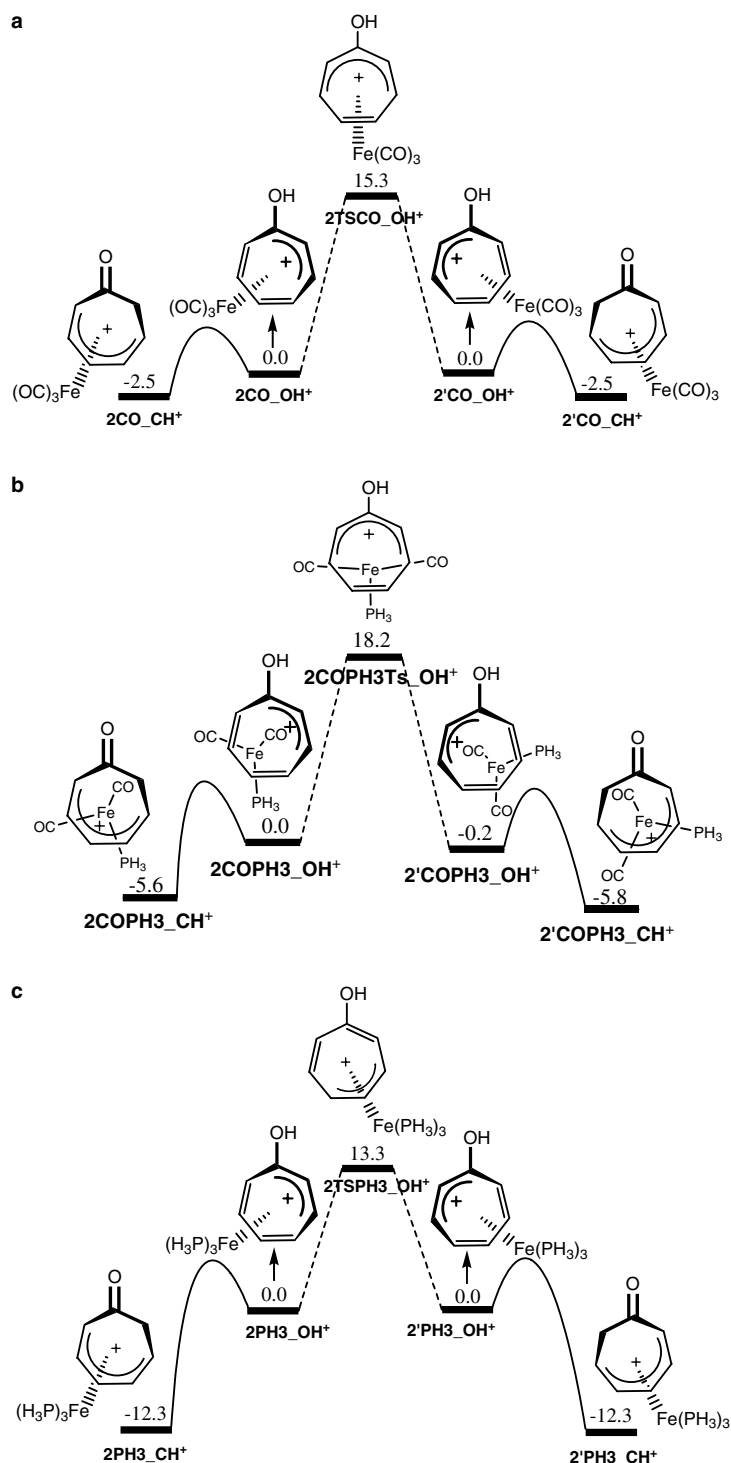

Fig. 6. Energy profiles of the metal shifts for protonated troponeiron complexes. The relative energies are given in kcal/mol.

states **2TsCO** and **2TsCOPH3**, are η^2-coordinated. In contrast, the oxygen-protonated tropone ligand in the transition state **2TsPH3_OH$^+$** is calculated to be η^3-coordinated.

In Fig. 6, we also illustrate schematically the interconversion between carbon- and oxygen-protonated species. The interconversion, which resembles an enol-to-keto tautomerization process [27] commonly found in organic chemistry, is expected to have a very small barrier in an acidic media. The evaluation of enol-to-keto tautomerization process (an intermolecular mechanism) requires enormous efforts computationally because solvation effects are the most important factor influencing the proton transfer process. Therefore, we did not calculate the interconversion barrier, which is commonly believed to be small.

From Fig. 6, one can easily find that an increase in the number of the phosphine ligands leads to higher stability of the carbon-protonated species with respect to the oxygen-protonated species. Due to the fast conversion from an oxygen-protonated species to its carbon-protonated isomer because of the small barrier commonly found in an enol-to-keto tautomerization, the overall barrier for the metal shift of a given protonated complex should be the energy difference between the summit and trough of the energy profile under consideration (Fig. 6), which was defined as the energetic span in the literature [28]. As a result, the barriers of the metal shifts (interconversion between two carbon protonated complexes) for complexes containing phosphine ligand(s) are much greater when compared with that for the complex containing only carbonyl ligands (23.8 and 25.6 kcal/mol for **2COPH3_CH$^+$** and **2PH3_CH$^+$**, respectively, versus 17.8 kcal/mol for **2CO_CH$^+$**). These results can explain why it was experimentally found that the rate of the metal shift for (tropone)Fe(CO)$_2$(PPh$_3$) after protonation is considerably reduced. The presence of the relatively weak π-accepting phosphine ligands helps strengthen the bonds between the iron center and the η^5-coordinated carbon-protonated tropone ligand, leading to the deceleration of the metal shift.

3.3. Effects of tropone ring substituents

As mentioned in Section 1, the regioisomer **4** of the 2-methyltroponeiron complex was found experimentally to be more stable than the regioisomer **4′**. Similarly, the regioisomer **5** of the 2,6-dimethyltroponeiron complex was found to be more stable than the regioisomer **5′**. To understand the reason behind this, we optimized the regioisomers for both complexes. We found that **4** and **5** are by about 3.6 and 2.9 kcal/mol more stable than **4′** and **5′**, respectively (Fig. 7). These values are in fairly good agreement with the experimental findings that **4** and **5** are by about 2.1 and 2.0 kcal/mol more stable than **4′** and **5′**, respectively. Examining the optimized structural parameters (Fig. 7), we can see that among the carbon atoms involved in the metal–tropone bonding interactions (C2, C3, C4, and C5 in **4** and **5** and C4, C5, C6 and C7 in **4′** and **5′**) the C7 atoms in **4′** and **5′** have the weakest metal–carbon interac-
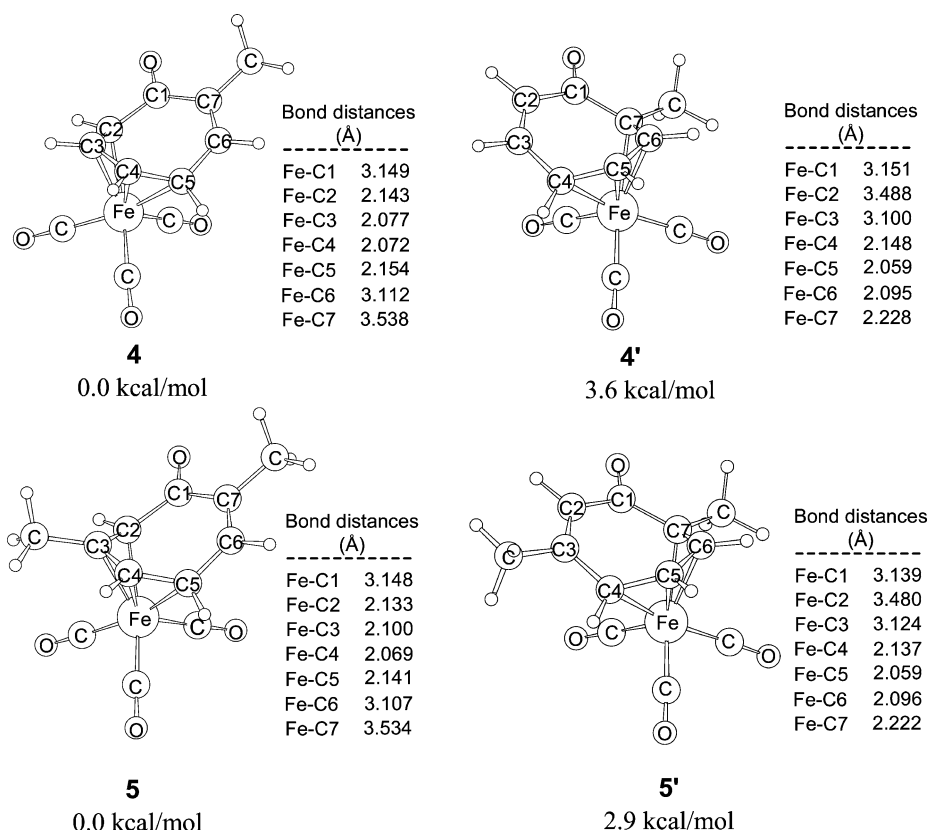

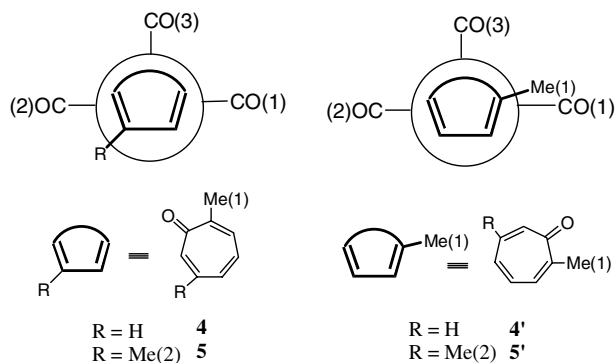Fig. 7. Optimized structures of the 2-methyltroponeiron and 2,6-dimethyltroponeiron complexes.

Fig. 8. Newman projection diagrams for the regioisomers of the 2-methyltroponeiron and 2,6-dimethyltroponeiron complexes.

Fig. 9. Optimized structures of the 2-tert-butyl-6-methyltroponeiron and 6-methyltroponeiron complexes.

tions evidenced by the longer Fe–C7 bond distances. Fig. 8 illustrates the Newman projection diagrams for the regioisomers of the two troponeiron complexes. In 4′ and 5′, greater repulsive interactions are expected between one of the carbonyl ligands (CO(1)) and one of the methyl groups (Me(1)) on the tropone ligand, resulting in the instability of these regioisomers. The repulsive interactions between CO(3) and the nearby substituents on the tropone ring are not significant because those ring carbons having the
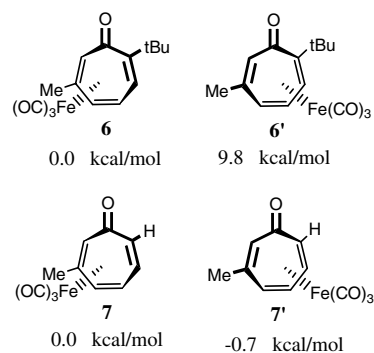
nearby substituents do not have bonding interactions with the metal center. To further support the argument here, we extended our calculations to the model complexes in which the Me(1) substituent in 5 or 5′ are replaced by t-Bu and H substituents, giving the regioisomers 6 or 6′ and 7 or 7′, respectively (Fig. 9). We can see from Fig. 9 that in comparison with 5 and 5′, the energy difference between 6 and 6′ increases and reaches 9.8 kcal/mol. On the contrary, our calculations show that 7′ is even more stable than 7
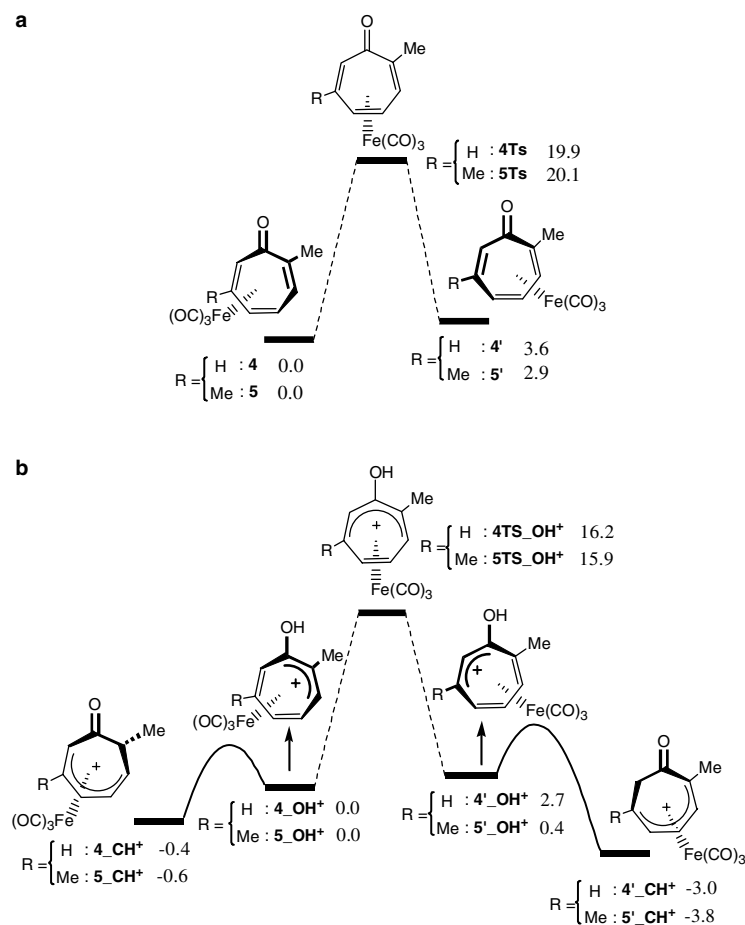

Fig. 10. Energy profiles of the metal shifts for the 2-methyltroponeiron, 2,6-dimethyltroponeiron and their protonated complexes. The relative energies are given in kcal/mol.

because the steric hindrance is minimized. These results support the argument that the steric factor determines the instability of **4′** and **5′**.

Energy profiles calculated for the 1,3 metal shifts of **4** and **5** are compared in Fig. 10a. The calculated barrier of the 1,3 metal shift for **4** (19.9 kcal/mol) is only ca. 0.2 kcal/mol lower than that for **5** (20.1 kcal/mol). The barriers obtained from the NMR experiments are 24.1 kcal/mol for **4** and 27.6 kcal/mol for **5** [2].

Fig. 10b compares the energy profiles calculated for the metal shifts for the protonated species of **4** and **5**. Consistent with the experimental findings that the protonated species of **4′** and **5′** are thermodynamically more stable than the protonated species of **4** and **5**, our calculations show that the carbon-protonated species of **4′** and **5′** are by about 2.6 and 3.2 kcal/mol more stable than the carbon-protonated species of **4** and **5**, respectively. The relative stability of 4_CH^+ versus $4'\_CH^+$, 5_CH^+ versus $5'\_CH^+$, 4_OH^+ versus $4'\_OH^+$, and 5_OH^+ versus $5'\_OH^+$ can be understood when we consider the electron-donating properties of the methyl substituent(s) on the tropone ring. The methyl substituents are capable of stabilizing the positive charge carried by the complexes. The Lewis structures shown in Fig. 10b represent the best description regarding on which ring carbons the charge should be delocalized. For a given isomeric pair, the isomer having a Lewis structure in which the positive charge can be directly stabilized by the methyl substituent(s) is more stable. For example, comparing 4_CH^+ and $4'\_CH^+$, we see that the positive charge in the Lewis structure of $4'\_CH^+$ can be directly stabilized by the methyl substituent while the positive charge in 4_CH^+ cannot be directly stabilized. 5_OH^+ and $5'\_OH^+$ have similar stability. In the Lewis structures representing 5_OH^+ and $5'\_OH^+$, the charge can be directly stabilized by a methyl substituent.

4. Summary

Structures and stabilities of tropone and troponeiron complexes, $(tropone)Fe(CO)_3$, $(tropone)Fe(CO)_2(PH_3)$ and $(tropone)Fe(PH_3)_3$, and their protonated species have been theoretically investigated. The results of our calculations show that while the oxygen-protonated tropone is more stable than the carbon-protonated tropone, the carbon-protonated species of the troponriron complexes are more stable. The higher stability of the oxygen-protonated tropone versus the carbon-protonated tropone was attributed to aromaticity of the oxygen-protonated tropone. In the neutral and oxygen-protonated complexes, the tropone and oxygen-protonated tropone ligands are η^4-coordinated with the metal center. In contrast, in the carbon-protonated complexes, the carbon-protonated tropone ligand is η^5-coordinated. The NBO analyses demonstrated that among the three ligands, the tropone, the oxygen-protonated and the carbon-protonated ligands, the carbon-protonated ligand is the strongest electron acceptor. For a given protonated complex, the high stability of the carbon-protonated species is due to the η^5-coordination of the carbon-protonated tropone ligand as well as the greater delocalization of the positive charge over the metal fragments FeL_3.

The calculations also indicated that the energy difference between the carbon- and oxygen-protonated species increases with the number of the phosphine ligands. Presence of the weaker π-accepting phosphine ligands in comparison with the carbonyl ligands allows much more electron transfer from the metal fragment to the carbon-protonated tropone ligand and in turn gives the stable carbon-protonated species.

The metal shift of the neutral and protonated tropone complexes was also studied. For protonated complexes containing phosphine ligand(s), the metal shift was found to be more difficult due to the high stability of the corresponding carbon-protonated species.

We also extended our study to the troponeiron complexes having Me substituent(s) on the tropone ring. For the neutral methyl-substituted troponeiron complexes, it was concluded that the relative stability among different regioisomers of the methyl-substituted troponeiron complexes is mainly governed by steric factor (repulsion between one of the carbonyl ligands and the nearby Me substituent(s) on the tropone ring). For the methyl-substituted protonated troponeiron complexes, electron-donating properties of the methyl substituent(s) determine the relative stability of the regioisomers.

Acknowledgments

References

[1] (a) M. Rosenblum, J.C. Watkins, J. Am. Chem. Soc. 112 (1990) 6316;
(b) M. Ohkita, S. Nishida, T. Tsuji, J. Am. Chem. Soc. 121 (1999) 4589;
(c) B. Horváth, A. Boháč, M. Sališová, E. Solčániová, M. Rosenblum, J. Organomet. Chem. 659 (2002) 43;
(d) Y. Coquerel, J.-P. Deprés, A.E. Greene, C. Philouze, J. Organomet. Chem. 659 (2002) 176;
(e) Y. Yoshitake, H. Nakagawa, M. Eto, K. Harano, Tetrahedron Lett. 41 (2000) 4395;
(f) J. Soulié, J.-F. Betzer, B. Muller, J.-Y. Lallemand, Tetrahedron Lett. 52 (1995) 9485;
(g) A.J. Pearson, K. Srinivasan, J. Org. Chem. 57 (1992) 3965;
(h) M.-C.P. Yeh, C.-C. Hwu, C.-H. Ueng, H.-L. Lue, Organometallics 13 (1994) 1788;
(i) J.H. Rigby, S.D. Rege, V.P. Sandanayaka, M. Kirova, J. Org. Chem. 61 (1996) 842;
(j) K. Saito, S. Ando, Y. Kondo, Heterocycles 53 (2000) 2601;
(k) M. Nitta, Y. Tajima, J. Chem. Res. Synop. 6 (1999) 372;
(l) K. Kumar, A. Kapur, M.P.S. Ishar, Org. Lett. 2 (2000) 787.
[2] A. Almássy, B. Horváth, A. Boháč, M. Sališová, G. Addová, M. Rosenblum, J. Organometal. Chem. 689 (2004) 1131.
[3] J.A.S. Howell, A.D. Squibb, Z. Goldschmidt, H.E. Gottlieb, A. Almadhoun, I. Goldberg, Organometallics 9 (1990) 80.
[4] N. Morita, M. Kurita, S. Ito, T. Asao, H. Sotokawa, A. Tajiri, Tetrahedron: Asymm. 6 (1995) 35.

[5] Y. Lou, Y. He, J.T. Kendall, D.M. Lemal, J. Org. Chem. 68 (2003) 3891.

[6] H. Hosoya, S. Nagakura, Bull. Chem. Soc. Jpn. 39 (1966) 1414.

[7] M.S. Brookhart, C.P. Lewis, A. Eisenstadt, J. Organometal. Chem. 127 (1977) C14.

[8] A. Eisenstadt, S. Winstein, Tetrahedron Lett. 7 (1971) 613.

[9] D.F. Hunt, G.C. Farrant, G.T. Rodeheaver, J. Organometal. Chem. 38 (1972) 349.

[10] (a) A.D. Becke, J. Chem. Phys. 98 (1993) 5648;
(b) B. Miehlich, A. Savin, H. Stoll, H. Preuss, Chem. Phys. Lett. 157 (1989) 200;
(c) C. Lee, W. Yang, G. Parr, Phys. Rev. B37 (1988) 785.

[11] P.C. Hariharan, J.A. Pople, Theor. Chim. Acta 28 (1973) 213.

[12] (a) P.J. Hay, W.R. Wadt, J. Chem. Phys. 82 (1985) 270;
(b) W.R. Wadt, P.J. Hay, J. Chem. Phys. 82 (1985) 284;
(c) P.J. Hay, W.R. Wadt, J. Chem. Phys. 82 (1985) 299.

[13] S. Huzinaga, Gaussian Basis Sets for Molecular Calculations, Elsevier Science Publishing Co., Amsterdam, 1984.

[14] A.W. Ehlers, M. Bohme, S. Dapprich, A. Gobbi, A. Hollwarth, V. Jonas, K.F. Kohler, R. Stegmann, A. Veldkamp, G. Frenking, Chem. Phys. Lett. 208 (1993) 111.

[15] (a) K. Fukui, J. Phys. Chem. 74 (1970) 4161;
(b) K. Fukui, Acc. Chem. Res. 14 (1981) 363.

[16] E.D. Glendening, A.E. Read, J.E. Carpenter, F. Weinhold, NBO (version 3.1), Gaussian, Inc., Pittsburg, PA, 1998.

[17] P.v.R. Schleyer, C. Maerker, A. Dransfeld, H. Jiao, N.J.R.v.E. Hommes, J. Am. Chem. Soc. 118 (1996) 6317.

[18] K. Wolinski, J.F. Hinton, P. Pulay, J. Am. Chem. Soc. 112 (1990) 8251.

[19] (a) A. Bergner, M. Dolg, W. Kuechle, H. Stoll, H. Preuss, Mol. Phys. 80 (1993) 1431;
(b) M. Dolg, U. Wedig, H. Stoll, H. Preuss, J. Chem. Phys. 86 (1987) 866.

[20] M.J. Frisch, G.W. Trucks, H.B. Schlegel, G.E. Scuseria, M.A. Robb, J.R. Cheeseman, J.A. Montgomery Jr., T. Vreven, K.N. Kudin, J.C. Burant, J.M. Millam, S.S. Lyengar, J. Tomasi, V. Barone, B. Mennucci, M. Cossi, G. Scalmani, N. Rega, G.A. Petersson, H. Nakatsuji, M. Hada, M. Ehara, K. Toyota, R. Fukuda, J. Hasegawa, M. Ishida, T. Nakajima, Y. Honda, O. Kitao, H. Nakai, M. Klene, X. Li, J.E. Knox, H.P. Hratchian, J.B. Cross, C. Adamo, J. Jaramillo, R. Gomperts, R.E. Stratmann, O. Yazyev, A.J. Austin, R. Cammi, C. Pomelli, J. Ochterski, P.Y. Ayala, K. Morokuma, G.A. Voth, P. Salvador, J.J. Dannenberg, V.G. Zakrzewski, S. Dapprich, A.D. Daniels, M.C. Strain, O. Farkas, D.K. Malick, A.D. Rabuck, K. Raghavachari, J.B. Foresman, J.V. Ortiz, Q. Cui, A.G. Baboul, S. Clifford, J. Cioslowski, B.B. Stefanov, G. Liu, A. Liashenko, P. Piskorz, I. Komaromi, R.L. Martin, D.J. Fox, T. Keith, M.A. Al-Laham, C.Y. Peng, A. Nanayakkara, M. Challacombe, P.M.W. Gill, B. Johnson, W. Chen, M.W. Wong, C. Gonzalez, J.A. Pople, GAUSSIAN 03, Gaussian, Inc., Pittsburgh, PA, 2003.

[21] R.W.A. Havenith, P.W. Fowler, E. Steiner, J. Chem. Soc., Perkin Trans. 2 (2002) 502.

[22] D. Lioyd, Non-Benzenoid Conjugated Carbocyclic Compounds, Elsevier, New York, 1984, p. 70.

[23] A. Ariafard, Z. Lin, Organometallics 24 (2005) 3800.

[24] (a) K.J. Karel, T.A. Albright, M. Brookhart, Organometallics 1 (1982) 419;
(b) M.G. Banwell, H.M. Schuhbauer, Organometallics 15 (1996) 4078.

[25] A. Tajiri, N. Morita, T. Asao, M. Hatano, Angew. Chem., Int. Ed. Engl. 24 (1985) 329.

[26] Ò. González-Blanco, V. Branchadell, Organometallics 19 (2000) 4078.

[27] (a) F.A. Carey, R.J. Sundberg, Advanced Organic Chemistry, Part A: Structure and Mechanisms, third ed., Plenum Press, New York, 1990, pp. 416–422;
(b) J.P. Guthrie, in: Z. Rappoport (Ed.), The Chemistry of Enols, Wiley, New York, 1990, pp. 75–93;
(c) J. Toullec, in: Z. Rappoport (Ed.), The Chemistry of Enols, Wiley, New York, 1990, pp. 323–398;
(d) J.R. Keeffe, A.J. Kresge, in: Z. Rappoport (Ed.), The Chemistry of Enols, Wiley, New York, 1990, pp. 399–480.

[28] S. Kozuch, C. Amatore, A. Jutand, S. Shaik, Organometallics 24 (2005) 2319.